Investigation of dipole excitations in ^{142}Ce using resonant photon scattering

A. Gade,[1,*] N. Pietralla,[1,2] P. von Brentano,[1] D. Belic,[3] C. Fransen,[1] U. Kneissl,[3] C. Kohstall,[3] A. Linnemann,[1] H. H. Pitz,[3] M. Scheck,[3] N. A. Smirnova,[4] F. Stedile,[3] and V. Werner[1]

[1]*Institut für Kernphysik der Universität zu Köln, Zülpicher Strasse 77, D-50937 Köln, Germany*

[2]*Department of Physics and Astronomy, State University of New York at Stony Brook, Stony Brook, New York 11794*

[3]*Institut für Strahlenphysik, Universität Stuttgart, Allmandring 3, D-70569 Stuttgart, Germany*

[4]*Department of Subatomic and Radiation Physics, University of Ghent, Proeftuinstraat 86, B-9000 Ghent, Belgium*

(Received 3 November 2003; published 27 May 2004)

A photon scattering experiment with bremsstrahlung has been performed on the vibrational nucleus ^{142}Ce up to a photon endpoint energy of 4.1 MeV. Fourteen dipole excitations have been observed between 2.1 and 3.9 MeV, five of them for the first time. A candidate for the 1^- dipole member of the recently proposed quintuplet of negative parity $(2^+_{1,\mathrm{ms}} \otimes 3^-_1)^{(J^-)}$, involving the $2^+_{1,\mathrm{ms}}$ isovector quadrupole excitation in the valence shell, has been identified. This exotic 1^-_{ms} state has been predicted within the sdf-IBM-2 and is expected to be accessible to photon scattering measurements. Solely one of nine $J=1$ states in the energy region of interest shows a decay pattern compatible with the model predictions for the 1^-_{ms} state.

DOI: 10.1103/PhysRevC.69.054321 PACS number(s): 21.10.Re, 21.60.Fw, 23.20.Lv, 27.60.+j

I. INTRODUCTION

Low-lying quadrupole and octupole vibrations dominate the excitation pattern of near spherical even-even nuclei. The first excited 3^- state can be understood as the manifestation of the vibrational octupole degree of freedom. The fundamental building blocks of quadrupole vibrations are the well-known isoscalar 2^+_1 state and the isovector quadrupole excitation in the valence shell, the so-called $2^+_{1,\mathrm{ms}}$ (mixed-symmetry) state. Aside from "particlelike" intruder states occurring in some mass regions, the 2^+_1 state is the lowest-lying collective excitation in all even-even nuclei. The $2^+_{1,\mathrm{ms}}$ state contains antisymmetric parts with respect to the proton-neutron contribution in the wave function and is usually shifted to considerably higher excitation energy in comparison to the yrast 2^+ state.

Quadrupole-octupole coupled states have been extensively investigated during the last decades. Especially the isoscalar quadrupole-octupole coupled dipole mode $(2^+_1 \otimes 3^-)^{(1^-)}$ attracted much attention in magic and near spherical nuclei [1–7]. The structure mentioned above involves the isoscalar 2^+_1 state and immediately questions the existence of the isovector analog $(2^+_{1,\mathrm{ms}} \otimes 3^-)$. Identification of multiphonon structures with mixed symmetry, i.e., with isovector excitation character in the valence shell, is important for judging the capability of the $2^+_{1,\mathrm{ms}}$ state to act as a building block of nuclear structure and, consequently, for our understanding of the impact of the proton-neutron degree of freedom on the formation of nuclear collectivity.

Mixed-symmetry two-phonon structures of the type $(2^+_1 \otimes 2^+_{1,\mathrm{ms}})$ have recently been unambiguously identified [8–10] on the basis of absolute $M1$ transition matrix elements. Such structures were subsequently studied in several nuclei [11–14]. The mixed-symmetry multiplet of negative parity $(2^+_{1,\mathrm{ms}} \otimes 3^-_1)^{(J^-)}$, $J=1,2,3,4,5$ has been suggested recently in the framework of the sdf-IBM-2 [15], the octupole extension of the proton-neutron interacting boson model [16] to the sdf space. Analytical expressions for its excitation energy and decay properties were derived [15]. In a simple harmonic coupling scheme one expects this multiplet to exist at about the sum energy $E(J^-_{\mathrm{ms}})=E(2^+_{1,\mathrm{ms}})+E(3^-_1)$. Recent observation of the electromagnetic coupling between the 3^- octupole phonon state and the $2^+_{1,\mathrm{ms}}$ mixed-symmetry quadrupole phonon excitation through an enhanced $E1$ transition [17] has provided direct evidence for the predominantly isovector character of the effective $E1$ operator in the valence shell and constrains the parameters of the $E1$ operator in the sdf-IBM-2. These constraints [17] and the analytic expressions from Ref. [15] can be used to quantify our expectations for the absolute and relative $E1$ decay rates of two-phonon negative-parity states with mixed proton-neutron symmetry. Such quantitative predictions for the decay rates and branching ratios can serve us in identifying fragments of the corresponding collective modes.

In the near-spherical nucleus ^{142}Ce several "key states" of the sdf-IBM-2 are known: the quadrupole and octupole one-phonon states, two fragments of the mixed-symmetry $2^+_{1,\mathrm{ms}}$ one-phonon state, and members of the symmetric $(2^+_1 \otimes 3^-_1)$ quadrupole-octupole coupled two-phonon multiplet [18–20]. Moreover, the γ-transition strength between the 3^-_1 state and one fragment of the $2^+_{1,\mathrm{ms}}$ state is known [17,18]. In ^{142}Ce the two main fragments of the $2^+_{1,\mathrm{ms}}$ excitation have been identified at 2004 and 2365 keV [18] while the 3^-_1 state is relatively low lying with an excitation energy of 1653 keV. Therefore, the first J^-_{ms} two-phonon quintuplet is expected in the harmonic scheme to exist at about 3.8 MeV excitation energy. The 1^-_{ms} dipole member of this quintuplet is supposed to decay predominantly to the 2^+_1 state and with sizable $E1$ strength to the ground state. The expected $E1$ rates should be comparable to those from other quadrupole-octupole coupled states. Indeed, several $E1$ transition rates between low-lying states can be quantitatively reproduced [17] within the

*Present address: NSCL, Michigan State University, East Lansing, MI 48824, USA.

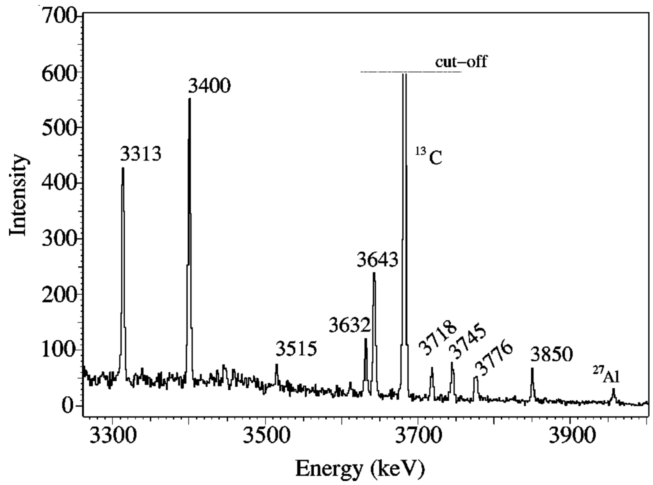

FIG. 1. Part of the NRF spectrum observed at a scattering angle of 127° with a Compton-escape suppressed HPGe detector. All peaks from ^{142}Ce are labeled with their energy. Transitions stemming from the calibration standards are also marked.

sdf-IBM-2 with a simple choice for the effective $E1$ transition operator. The model makes then quantitative predictions [15] for the quadrupole-octupole coupled states with mixed-symmetry character and negative parity. These predicted properties would make the 1^-_{ms} state accessible to the method of nuclear resonance fluorescence (NRF) at the Stuttgart 4.3 MV DYNAMITRON accelerator [21].

Previous knowledge on the excitation spectrum of ^{142}Ce stems from Coulomb excitation [19,22], β decay [23,24], and electron scattering [25]. In 1995, ^{142}Ce was investigated using inelastic neutron scattering $(n,n'\gamma)$, resulting also in lifetime information on spin 1 states up to 3.3 MeV [18]. Data on higher excited states with $J=1$ were still rare and motivated our NRF study on ^{142}Ce.

II. EXPERIMENT

Resonant photon scattering is known as a well-suited experimental method to induce dipole and quadrupole excitations that are connected to the ground state by sufficient excitation matrix elements [21]. In that sense, this experimental probe is spin and strength selective and the method of choice to look for the 1^-_{ms} excitation in ^{142}Ce. A photon scattering experiment was performed at the bremsstrahlung facility of the DYNAMITRON accelerator in Stuttgart. The target consisted of 1083 mg CeO_2 with an enrichment of 91.5% in ^{142}Ce and additionally 506 mg ^{27}Al and 70 mg ^{13}C for photon flux calibration purposes. The experiment took about 100 h at an endpoint energy of the bremsstrahlung spectrum of 4.1 MeV. Figure 1 shows a part of the photon scattering spectrum of ^{142}Ce observed with a Compton-shielded HPGe detector at a scattering angle of 127°.

Sharp peaks appear above the smooth nonresonant background. These peaks stem from the decays of the resonantly excited states. For some states it was possible to observe the transition to the ground state as well as to the 2^+_1 state at 641 keV. The measured decay intensities yield the ratio Γ_1/Γ_0 of the partial widths for the decays to the 2^+_1 and the ground state, respectively. The observation of decays to higher excited states than the 2^+_1 is usually prevented by the rapidly increasing nonresonant background towards lower energies in the spectra.

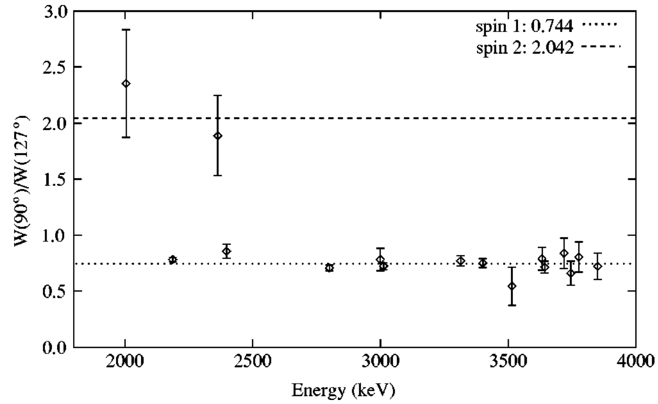

FIG. 2. Angular distribution of ground-state transitions $J^\pi \to 0^+_1$ in ^{142}Ce. The intensity ratio $W(90°)/W(127°)$ enables us to assign 14 $J=1$ and two $J=2$ spin quantum numbers, five of them for the first time.

The experimental setup [21] provided the possibility to determine spin values with the method of angular distributions. Three HPGe detectors were positioned at 90°, 127°, and 150° with respect to the beam axis. The intensity ratio $W(90°)/W(127°)$ is sensitive to distinguish spin $J=1$ and $J=2$ quantum numbers in even-even nuclei. Figure 2 shows the observed intensity ratios, $W(90°)/W(127°)$, for ^{142}Ce

TABLE I. Results from the NRF measurement of ^{142}Ce. Observed branching ratios and reduced branching ratio $R=(\Gamma_1 E^3_{\gamma_0})/(\Gamma_0 E^3_{\gamma_1})$ for the decay to the 2^+_1 state, decay widths, and scattering cross sections are given. For the states at 3314, 3633, 3719, and 3850 keV additional branchings were reported in the mid-1980's [36]. However, in our data there is no evidence even for the strongest of these reported decays which should be accessible to our technique. They are therefore not included in our analysis.

E_i (keV)	J^π ($\hbar$)	Γ_1/Γ_0	R	I_s (eV b)	Γ_0 (meV)	τ (fs)
2187.0	1^-	0.63(2)	1.78(6)	59.0(19)	39.8(14)	10.2(4)
2397.8	1^+	0.24(5)	0.61(13)	12.0(5)	7.41(44)	72(4)
2800.8	$1^{(+)}$	0.19(2)	0.41(14)	36.8(13)	29.9(12)	18.4(7)
2999.7	1	1.65(12)	3.39(25)	5.8(3)	11.9(9)	21(2)
3012.5	1	…		28.4(10)	22.4(8)	29.4(10)
3313.8	1	0.21(3)	0.40(6)	24.5(9)	28.3(13)	19.2(9)
3400.9	1	…		33.4(12)	33.6(12)	19.6(7)
3515.1	1	1.10(21)	2.0(4)	2.9(3)	6.7(10)	47^{+9}_{-6}
3632.6	1	…		10.8(7)	12.32(71)	53(3)
3643.4	1	…		25.6(11)	29.5(12)	22(1)
3718.8	1	…		9.4(7)	11.24(75)	59(4)
3745.7	1	…		10.0(8)	12.23(88)	54(4)
3776.6	1	…		11.0(8)	13.6(10)	48(4)
3850.2	1	…		15.7(12)	20.3(16)	32(3)

TABLE II. Absolute transition strengths of $J=1$ states in ^{142}Ce. In the case of unknown radiation character the values for all possible (pure) multipolarities are given. In addition, level energy E_i, initial and final spins J_i^π and J_f^π, the γ-ray transition energy E_γ, and the reduced branching ration R are listed.

E_i (keV)	J_i^π ($\hbar$)	R	E_γ (keV)	J_f^π ($\hbar$)	$B(E1;J_i^\pi\to J_f^\pi)$ ($10^{-3}e^2$ fm^2)	$B(M1;J_i^\pi\to J_f^\pi)$ (μ_N^2)	$B(E2;J_i^\pi\to J_f^\pi)$ (e^2 fm^4)
2187.0	1^-	1.78(6)	2187.0	0_1^+	3.62(12)		
			1545.7	2_1^+	6.45(33)		
2397.8	1^+	0.61(13)	2397.8	0_1^+		0.047(3)	
			1756.5	2_1^+		0.028(6)	132(28)
2800.8	$1^{(+)}$	0.41(4)	2800.8	0_1^+		0.118(7)	
			2159.5	2_1^+		0.049(5)	151(17)
2999.7	1	3.39(25)	2999.7	0_1^+	0.42(6)	0.038(5)	
			2358.4	2_1^+	1.4(2)	0.13(1)	332(37)
3012.5	1	0.0	3012.5	0_1^+	0.78(3)	0.071(3)	
3313.8	1	0.40(6)	3313.8	0_1^+	0.74(4)	0.067(3)	
			2672.5	2_1^+	0.30(6)	0.027(5)	54(11)
3400.9	1	0.0	3400.9	0_1^+	0.82(3)	0.074(3)	
3515.1	1	2.0(4)	3515.1	0_1^+	0.15(3)	0.013(3)	
			2873.8	2_1^+	0.30(7)	0.027(5)	47(10)
3632.6	1	0.0	3632.6	0_1^+	0.24(2)	0.022(2)	
3643.4	1	0.0	3643.4	0_1^+	0.58(3)	0.053(2)	
3718.8	1	0.0	3718.8	0_1^+	0.21(2)	0.019(1)	
3745.7	1	0.0	3745.7	0_1^+	0.22(2)	0.020(1)	
3776.6	1	0.0	3776.6	0_1^+	0.24(2)	0.022(1)	
3850.2	1	0.0	3850.2	0_1^+	0.34(3)	0.031(3)	

along with the expectation values for spin assignments $J=1$ or 2 for the photoexcited states. Absolute energy-integrated resonance scattering cross sections

$$I_{s,0} = g\pi^2\lambda\!\!\!^{-2}\frac{\Gamma_0^2}{\Gamma} \tag{1}$$

of the states in ^{142}Ce were obtained relative to the well-known [26] cross sections of several states in ^{27}Al and ^{13}C. Here, $g=(2J+1)/(2J_0+1)$ is a statistical factor, $\lambda\!\!\!^{-2}=\hbar c/E_x$ is the reduced excitation wavelength, and $\Gamma(\Gamma_0)$ denotes the total (partial) decay width of the level (for the decay back to the ground state). From the cross section, $I_{s,0}$, and relative widths, Γ_0/Γ, total level lifetimes

$$\tau = \frac{\hbar}{\Gamma} = \frac{g\pi^2\lambda\!\!\!^{-2}\hbar^2}{I_{s,0}}\left(\frac{\Gamma_0}{\Gamma}\right)^2$$

of the resonantly excited states can be deduced model independently.

We observed nine dipole excitations between 3.3 and 3.9 MeV, five of them for the first time. Tables I and II summarize the NRF results. We list excitation energy, spin and parity assignment, intensity branching ratio and the reduced branching ratio $R=(\Gamma_1 E_{\gamma_0}^3)/(\Gamma_0 E_{\gamma_1}^3)$ for the decay to the 2_1^+ state, integrated scattering cross section I_s, the partial width for the decay to the ground state Γ_0, and the resulting level lifetime τ. It was possible to confirm known lifetimes for the states at 2187, 2398, 2801, 3000, and 3013 keV, partly with a significant reduction of the uncertainty. Due to low coincidence statistics caused by the lack of sufficient target material it was not possible to use the Compton polarimeter for the determination of parities.

III. DISCUSSION

In the energy region of interest the parities of the $J=1$ states are widely unknown. In Fig. 3 we compare the absolute transition strengths $B(\sigma1;1^\pi\to 0_1^+)$ measured in ^{142}Ce to the findings for the $N=84$ isotone ^{144}Nd for which parities are partly assigned at higher energies from Compton polarimetry in photon scattering [27].

Dipole excitations of both parities occur in the accessible energy region. We will comment on the presumed character of these states in the following subsections.

A. Magnetic dipole excitations

An interesting class of collective states has been predicted in the framework of the IBM-2, the so-called mixed-symmetry states. The wave functions of these excitations contain antisymmetric components with respect to the proton-neutron degree of freedom and their decay pattern is characterized by strong $M1$ transitions to proton-neutron symmetric states [28]. The study of such excitations is of great interest and serves us in better understanding the inter-

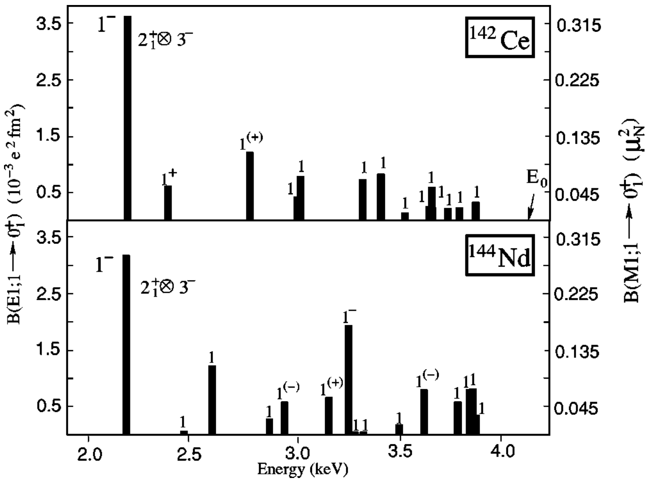

FIG. 3. Experimental $B(\sigma 1;1\rightarrow 0_1^+)$ dipole decay strength distributions for the neighboring even-even $N=84$ isotones ^{142}Ce and ^{144}Nd. The isoscalar $(2_1^+\otimes 3_1^-)^{(1^-)}$ state carries the dominant amount of $E1$ strength in the analyzed energy region in both nuclei.

play between protons and neutrons in the atomic nucleus. The most prominent mixed-symmetry state is the magnetic dipole 1^+_{ms} state, which is called "scissors mode" in deformed nuclei. This 1^+ state was discovered by Richter and coworkers in electron scattering experiments at Darmstadt [29]. The existence of mixed-symmetry 1^+_{ms} states has been systematically investigated in the $100<A<200$ mass region using the resonant photon scattering technique [21,30–32]. Photon scattering is particularly useful for the investigation of these states because in deformed nuclei the "scissors mode" is connected to the 0^+ ground state by a strong $M1$ transition matrix element. The mentioned systematics showed that this excitation is usually fragmented around 3 MeV with only little dependence on the nuclear deformation [31]. Under the extreme assumption that all observed dipole excitations of ^{142}Ce in the energy region $2.3\leqslant E\leqslant 3.5$ MeV would have positive parity, we can establish the upper limit of $0.43\mu_N^2$ for the decay $M1$ strength of the mixed-symmetry two-phonon 1^+ state of ^{142}Ce. Summing the absolute $B(\sigma 1;1^\pi\rightarrow 0_1^+)$ decay strength below 3.3 MeV in ^{142}Ce results then in $0.075\mu_N^2<\Sigma B(M1;1^+\rightarrow 0_1^+)<0.43\mu_N^2$. Due to the lacking parity information, we can expect, however, that the upper limit deduced above overestimates the actual value considerably. Of course the knowledge of the parity quantum numbers is necessary for a final assignment of the 1^+_{ms} fragments. For a near spherical nucleus the decay strength to the ground state is expected to be small compared to a well deformed nucleus. For ^{94}Mo, the currently best-studied nucleus for mixed-symmetry multiphonon structures, a corresponding value of $\Sigma B(M1;1^+\rightarrow 0_1^+)=0.22(3)\mu_N^2$ has been determined experimentally below 4 MeV [14]. Recent microscopic calculations for ^{142}Ce carried out in the framework of the random phase approximation predict the decay strength to be about 0.07 μ_N^2 [33]. This agrees well with systematic microscopic studies of mixed-symmetry structures in vibrational nuclei in the quasiparticle phonon model [34].

B. Electric dipole excitations

The study of the coupling of various collective excitations is of great interest in nuclear structure physics. The crucial question is to what extent the fundamental modes can be combined to form multiphonon structures. A particularly interesting problem is the coupling of the lowest quadrupole and octupole modes in nuclei. In a harmonic coupling scheme one expects the quintuplet of negative parity $(2_1^+\otimes 3_1^-)$ states to occur at the sum energy, $E(2_1^+)+E(3_1^-)$, of its constituents. The 1^- member of this multiplet at 2187 keV lies 107 keV below the sum energy and fits well into the systematic of quadrupole-octupole coupled 1^- excitations in this mass region [1,5].

A more exotic excitation mode results from the coupling of the fundamental $2^+_{1,\mathrm{ms}}$ excitation and the 3^- octupole state. This mixed-symmetry state of negative parity has been predicted in the framework of the sdf-IBM-2 but it has not yet been observed experimentally. Our data contains information on one $J=1$ state, which shows a decay branching ratio in agreement with the prediction for the 1^-_{ms} state. On this basis we propose this state as a promising candidate for the 1^-_{ms} excitation. In the following subsections we will briefly describe the algebraic sdf-IBM-2 model, discuss its relevant predictions for ^{142}Ce, and present a comparison to the data.

1. Quantitative application of the sdf-IBM-2

The underlying algebraic structure of the sdf-IBM-2 is $\mathrm{U}_\pi(13)\otimes\mathrm{U}_\nu(13)$. Its group reduction to the U(5) and SO(6) groups has been done in Ref. [15], where analytical expressions for energy eigenvalues, wave functions, and transition matrix elements have been derived. The proton-neutron symmetry of the wave functions is expressed in terms of the total F-spin quantum number, applied to the full set of s, d, and f bosons, and can further be classified into three categories with different symmetries in the sd-and f-boson subspaces [15].

The near-spherical nucleus ^{142}Ce was considered before as a reasonable example for the schematic, but analytically solvable, U(5) dynamical symmetry of the IBM [17,35]. We will discuss the decay properties of this nucleus in terms of the pure U(5) limit of the sdf-IBM-2. We consider here the schematic Hamiltonian

$$H=\epsilon_d C_1[\mathrm{U}_{\pi\nu}(5)]+\epsilon_f C_1[\mathrm{U}_{\pi\nu}(7)]+\gamma C_2[\mathrm{SO}_{\pi\nu}(3)] + \gamma_d C_2[\mathrm{SO}^d_{\pi\nu}(3)]+\lambda\hat{M}_{13}. \tag{2}$$

The definition of all operators and the full Hamiltonian of the sdf-IBM-2 in terms of Casimir operators can be found in Ref. [15]. We note that the full sdf-IBM-2 Hamiltonian can contain up to three independent Majorana operators for describing an energy splitting of mixed-symmetry states with different boson contents and coupling schemes. In order to restrict the number of parameters we consider only the leading term M_{13}. The energy eigenvalues are given by

$$E=\epsilon_d n_d+\epsilon_f n_f + \gamma_d L_d(L_d+1)+\gamma L(L+1) + \lambda[F_{\max}(F_{\max}+1)-F(F+1)], \tag{3}$$

where $F_{\max}=N/2$ and F denotes the total F spin of the boson

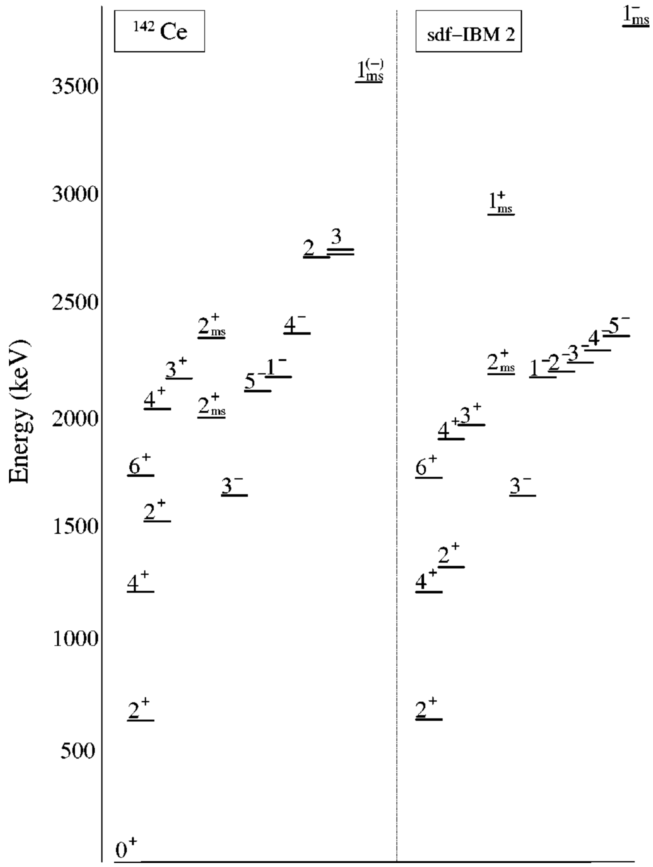

FIG. 4. Comparison of the experimental and calculated low-energy spectrum in the $\mathrm{U}(5)\otimes\mathrm{U}(7)$ dynamical symmetry limit. We used the set of parameters given in the text. The mixed-symmetry 2^+ state in ^{142}Ce is fragmented into two 2^+ states at 2 and 2.3 MeV. The experimental identification of the quadrupole-octupole coupled 2^- and 3^- states is unclear. We compare the spin 2 and two spin 3 states that are referred to as the most likely candidates for these excitations [18].

wave function. The experimental spectrum of ^{142}Ce [18] is shown in Fig. 4 in comparison with a spectrum of the $\mathrm{U}(5)\otimes\mathrm{U}(7)$ dynamical symmetry limit of the sdf-IBM-2 for the restricted Hamiltonian from Eq. (2) with the parameters

$$\epsilon_d = 688.7\ \text{keV},\quad \epsilon_f = 1572.8\ \text{keV},\quad \gamma_d = -14.58\ \text{keV},$$
$$\gamma = 6.68\ \text{keV},\quad \lambda = 312\ \text{keV},\ \text{and}\ N_\pi = 4,\quad N_\nu = 1.$$

Spin and parity quantum numbers were experimentally assigned to all known states of ^{142}Ce below about 2.7 MeV excitation energy. We compare the experimentally unambiguously identified positive-parity (multi)phonon states, the mixed-symmetry states, and the states with negative parity suggested to form the quadrupole-octupole coupled multiplet [18].

The symmetric quadrupole phonon 2_1^+ state is experimentally found at an excitation energy of $E(2_1^+)=641$ keV and the 3_1^- octupole phonon state is low lying at $E(3_1^-)=1653$ keV. The 1^- member of the proton-neutron symmetric $(2_1^+\otimes 3_1^-)$ quadrupole-octupole coupled two-phonon multiplet lies at an excitation energy of $E(1^-)=2187$ keV, which is close to the sum energy $E(2_1^+)+E(3_1^-)=2294$ keV of the constituents. ^{142}Ce is one of the few nuclei, for which, aside from the 1^- state, data on other members of the $(2_1^+\otimes 3_1^-)$ quintuplet are known. Based on the results of a neutron-scattering experiment Vanhoy *et al.* [18] assigned the 5_1^- state at 2125 keV and the 4_1^- state at 2385 keV to be of quadrupole-octupole coupled nature. These states are characterized by strong $E2$ transitions to the one-phonon octupole state and rather strong $E1$ transitions to the ground band. The assignment of 2^- and 3^- two-phonon states is less clear. The reason may be sizable mixing with noncollective configurations.

A fragment of the 2_{ms}^+ state, namely the 2_3^+ state at 2004 keV excitation energy, has been suggested first by Hamilton, Irbäck, and Elliott [35] and could be confirmed later by the measured large $M1$ transition strength [18,19]. The $(n,n'\gamma)$ data by Vanhoy *et al.* [18] suggest the short-lived 2_4^+ state at 2365 keV excitation energy as a further fragment of the 2_{ms}^+ state of ^{142}Ce, also based on the observation of a strong $M1$ transition to the 2_1^+ state.

In view of the restricted Hamiltonian (2) even in the pure U(5) dynamical symmetry limit, we must expect that it is unable to provide the optimum description within the framework of the IBM. However, the analytically solvable limit enables us to use analytical expressions [15] for a simple description of the data. Our goal here is, namely, to qualitatively reproduce the spectrum and decay pattern of known states in order to obtain a simple parameter set for predicting qualitatively the properties of the more "exotic" mixed-symmetry states with negative parity.

2. Transitions

Besides the energy spectrum, the model can quantitatively describe electromagnetic transition matrix elements by the consideration of effective boson transition operators. We use here the following transition operators:

$$T(E1) = \alpha_\pi D_\pi^{(1)} + \alpha_\nu D_\nu^{(1)} + \frac{\beta}{2N}\left[Q^{(2)}\left(\frac{e_\nu}{e_\pi}\right)\times O^{(3)}(\chi)\right]^{(1)},$$

$$T(E2) = e_\pi Q_\pi^{(2)}(\chi_\pi) + e_\nu Q_\nu^{(2)}(\chi_\nu),$$

$$T(E3) = e_3(O_\pi^{(3)}(\chi) + O_\nu^{(3)}(\chi)),$$

$$T(M1) = \sqrt{\frac{3}{4\pi}}(g_\pi L_\pi^d + g_\nu L_\nu^d), \tag{4}$$

where the multipole operators are described in detail in [15]. We stress that the sdf-IBM-2 for the first time enables a description of mixed-symmetry states and quadrupole-octupole coupling in a common algebraic approach. Of particular importance are transitions which are absent in the standard sd-IBM-2 or sdf-IBM-1, e.g., the F-vector $E1$ transitions [17].

We first outline the rationale of the fitting procedure for the effective parameters of the transition operators of the sdf-IBM-2 using the familiar language of collective phonon excitations. The corresponding quantitative data analysis within the *sdf*-IBM-2 provides then numerical values for the model parameters and thereby fixes the model predictions for hitherto unknown structures.

The effective charges for the proton and neutron parts of the $E2$ operator can be obtained from the $E2$ excitation strengths of the isoscalar and the isovector one-quadrupole phonon excitations. From the isovector $M1$ transition between them one can determine the difference of the effective g factors for proton and neutron bosons. We will accept the literature value $|g_\pi - g_\nu| = 1\mu_N$ [28]. The 1_1^- state decays by enhanced electric dipole transitions to the ground state and to the 2_1^+ state with relatively large $E1$ strengths of the order of $10^{-3}e^2$ fm^2. These $E1$ transition rates determine the two parameters of the quadrupole-octupole coupled two-body part of the $E1$ operator. The proton and neutron effective charges of the leading order one-body parts of the $E1$ operator are finally fixed from the reproduction of the isoscalar $3_1^- \to 2_1^+$ and isovector $3_1^- \to 2_{1,\mathrm{ms}}^+$ $E1$ transitions between the one-phonon excitations [17]. To be quantitative we use now the analytical expressions for the U(5) limit of the *sdf*-IBM-2 from Ref. [15] for finding an appropriate set of parameters for the transition operators (see Fig. 5).

In the U(5) limit we use standard values $\chi_\pi = \chi_\nu = 0$ for the structural parameters of the quadrupole operators Q_π and Q_ν. The ratio $\eta = e_\nu / e_\pi = 1/4$ of the effective quadrupole boson charges was adjusted to reproduce the experimental $E2$ excitation strength ratio $B(E2;0_1^+ \to 2_{\mathrm{ms}}^+)/B(E2;0_1^+ \to 2_1^+) = 0.11$ to the $F_{\max}$ and $F_{\max}-1$ one-quadrupole-phonon states. The $E1$ operator contains four free parameters. The $E1$ branching ratio, $B(E1;1_1^- \to 2_1^+)/B(E1;1_1^- \to 0_1^+) = 6\chi^2/25N = 1.78(6)$ (using R from Table I assuming pure $E1$ multipolarity for the $1^- \to 2_1^+$ transition) uniquely fixes the absolute value of $|\chi| = 6$. We use $\chi = -6$. The ground-state excitation strength $B(E1;0_1^+ \to 1^-_{(2_1^+ \otimes 3_1^-)})$ is a function of only β^2 and η [15]. Since the latter is known from $E2$ data, we can unambiguously obtain the absolute value $|\beta| = 0.08$ e fm. We use $\beta = -0.08$ e fm.

The parameters of the one-body terms, α_π and α_ν, can finally be fixed from the reproduction of the $B(E1;3_1^- \to 2_{\mathrm{ms}}^+)$ and $B(E1;3_1^- \to 2_1^+)$ values. We stress that the one-body part of the effective $E1$ operator turns out to have almost pure F-vector character [17]. Thus, the constraint $\alpha_\nu/\alpha_\pi = -1$ can be used to further reduce the number of free parameters for the description of $E1$ transition rates to three. The parameters and signs become unique if one poses the reasonable condition $N_\pi \alpha_\pi > |N_\nu \alpha_\nu| > 0$ with $N_\pi = 4$ and $N_\nu = 1$ for ^{142}Ce. These conditions result in the parameters $\alpha \equiv \alpha_\pi = -\alpha_\nu = 0.135$ e fm. Theoretical $E1$ transition rates using these three parameters of the $E1$ operator (α, β, χ) are compared to the data in Table III.

The octupole charge factor e_3 has been determined from the $B(E3;0_1^+ \to 3_1^-)$ value: it is $e_3 = 76$ e fm^3. For the $M1$ transition operator bare orbital values $g_\pi = 1$ μ_N and $g_\nu = 0$ for the boson g factors were used without any parameter adjustment. Some $B(E2)$ and $B(M1)$ values are listed in Table III.

The overall agreement between theoretical and experimental values is satisfactory. Although the observed strength of the $3_1^- \to 2_1^+$ $E1$ transition is unexpectedly small, it can be described simultaneously with the enhanced $E1$ transitions

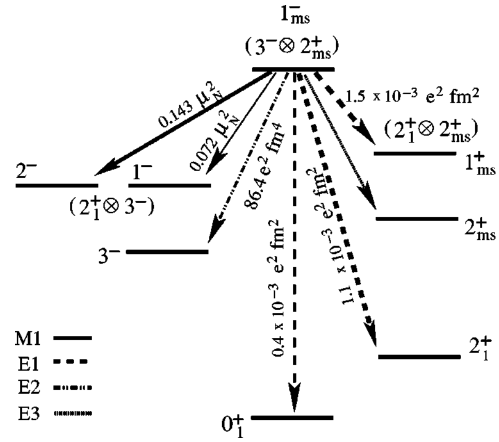

FIG. 5. Theoretical decay pattern of the 1_{ms}^- state predicted within the *sdf*-IBM-2. Given are the absolute $M1$, $E1$, and $E2$ transition strengths obtained from the parameter set discussed in the text.

from the 1_1^- state to the ground state and to the 2_1^+ state. The large $B(E1)$ value for the transition from the 3_1^- state to 2_2^+ is predicted, while this transition was not observed experimentally. The reason may be that since $E_\gamma(3_1^- \to 2_2^+) = 115.5$ keV, its intensity is much smaller than that of the $3_1^- \to 4_1^+$ transition with $E_\gamma = 433.5$ keV$[I \sim E_\gamma^3 B(E1)]$ and therefore escaped observation. The $B(E1;4_1^- \to 3_1^+)$ and $B(E1;5_1^- \to 4_1^+, 6_1^+)$ values are well reproduced. These transition strengths were not used to fit the parameters of the transition operator. They are, thus, predictions of the model and can be used to judge its predictive power. The only visible problem is the transition from 3_1^- state to 3_1^+, which is still outside the model, even when we apply a two-body $T(E1)$ operator. This interesting selection rule may be exploited to analyze a possible breaking of the assumed symmetries [F spin or U(5)].

3. Tentative assignment of a 1^-_{ms} *state*

With this working set of parameters one can have a look at predictions for the interesting mixed-symmetry states with negative parity. The relatively low-lying quintuplet of states, denoted by $(2_{\mathrm{ms}}^+ \otimes 3_1^-)$, is of particular interest, since both constituent one-phonon states are already known experimentally. In the harmonic phonon coupling scheme one expects this quintuplet of levels approximately at the sum energy, which is $E(2_{\mathrm{ms}}^+) + E(3_1^-) \approx 3.8$ MeV for ^{142}Ce.

The 1_{ms}^- shows one feature that distinguishes it from most of the other higher-lying dipole excitations and makes a tentative identification possible. The absolute transition strength $B(E1;1_{\mathrm{ms}}^- \to 0_1^+)$ only depends on $\beta^2(1-\eta)^2$:

$$B(E1;1_{\mathrm{ms}}^- \to 0_1^+) = \beta^2(1-\eta)^2 \frac{N_\pi N_\nu (N-2)}{N^2(N-1)}, \qquad (5)$$

while $B(E1;1_{\mathrm{ms}}^- \to 2_1^+)$ is also a function of χ^2:

$$B(E1;1_{\mathrm{ms}}^- \to 2_1^+) = \frac{6}{25}\beta^2\chi^2(1-\eta)^2 \frac{N_\pi N_\nu (N-2)}{N^3(N-1)}. \qquad (6)$$

In particular, one obtains for the $B(E1)$ ratio

TABLE III. Some experimental and theoretical transition strengths for ^{142}Ce. The parameters of the transition operators used for the calculation are specified in the text. The asterisks denote transition strengths, which were used to fit the model parameters as discussed in the text.

	Experimental (Present work and [18])	Theoretical
$B(E2;2_1^+\to 0_1^+)$	$924^{+88}_{-88}\ e^2\ \mathrm{fm}^4$	$1037\ e^2\ \mathrm{fm}^4$
$B(E2;2_2^+\to 2_1^+)$	$>836\ e^2\ \mathrm{fm}^4$	$1659\ e^2\ \mathrm{fm}^4$
$B(E2;2_{\mathrm{ms}}^+\to 0_1^+)$	$110^{+9}_{-9}\ e^2\ \mathrm{fm}^4$	$115\ e^2\ \mathrm{fm}^4$
$B(M1;2_{\mathrm{ms}}^+\to 2_1^+)$	$0.23^{+0.02}_{-0.02}\mu_N^2$	$0.23\mu_N^2$
$B(E3;0_1^+\to 3_1^-)^*$	$2.02^{+0.13}_{-0.13}\times 10^5 e^2\ \mathrm{fm}^6$	$2.02\times 10^5 e^2\ \mathrm{fm}^6$
$B(E1;3_1^-\to 2_1^+)$	$<0.21\times 10^{-3}e^2\ \mathrm{fm}^2$	$0.17\times 10^{-3}e^2\ \mathrm{fm}^2$
$B(E1;3_1^-\to 4_1^+)$	$<0.4\times 10^{-3}e^2\ \mathrm{fm}^2$	$0.33\times 10^{-3}e^2\ \mathrm{fm}^2$
$B(E1;3_1^-\to 2_2^+)$		$15.7\times 10^{-3}e^2\ \mathrm{fm}^2$
$B(E1;2_{\mathrm{ms}}^+\to 3_1^-)^*$	$4.6^{+0.5}_{-0.5}\times 10^{-3}e^2\ \mathrm{fm}^2$	$4.5\times 10^{-3}e^2\ \mathrm{fm}^2$
$B(E1;4_1^-\to 3_1^+)$	$4.4^{+37}_{-25}\times 10^{-3}e^2\ \mathrm{fm}^2$	$20.6\times 10^{-3}e^2\ \mathrm{fm}^2$
$B(E1;4_1^-\to 4_1^+)$	$0.74^{+0.70}_{-0.46}\times 10^{-3}e^2\ \mathrm{fm}^2$	$0.16\times 10^{-3}e^2\ \mathrm{fm}^2$
$B(E1;5_1^-\to 4_1^+)$	$<1.2\times 10^{-3}e^2\ \mathrm{fm}^2$	$0.96\times 10^{-3}e^2\ \mathrm{fm}^2$
$B(E1;5_1^-\to 6_1^+)$	$<1.7\times 10^{-3}e^2\ \mathrm{fm}^2$	$0.67\times 10^{-3}e^2\ \mathrm{fm}^2$
$B(E1;1_1^-\to 0_1^+)^*$	$3.6(1)\times 10^{-3}e^2\ \mathrm{fm}^2$	$3.7\times 10^{-3}e^2\ \mathrm{fm}^2$
$B(E1;1_1^-\to 2_1^+)^*$	$6.5(3)\times 10^{-3}e^2\ \mathrm{fm}^2$	$6.4\times 10^{-3}e^2\ \mathrm{fm}^2$
$B(E1;1_1^-\to 0_2^+)$		$0.45\times 10^{-3}e^2\ \mathrm{fm}^2$
$B(E1;1_1^-\to 2_2^+)$		$0.95\times 10^{-3}e^2\ \mathrm{fm}^2$
$B(E1;3_1^+\to 3_1^-)$	$0.44^{+0.33}_{-0.30}\times 10^{-3}e^2\ \mathrm{fm}^2$	0
$B(E1;(1_{\mathrm{ms}}^-)\to 0_1^+)$	$0.15(3)\times 10^{-3}e^2\ \mathrm{fm}^2$	$0.43\times 10^{-3}e^2\ \mathrm{fm}^2$
$B(E1;(1_{\mathrm{ms}}^-)\to 2_1^+)$	$0.30(7)\times 10^{-3}e^2\ \mathrm{fm}^2$	$0.75\times 10^{-3}e^2\ \mathrm{fm}^2$

$$R_{1^-_{\mathrm{ms}}} = \frac{B(E1;1^-_{\mathrm{ms}}\to 2^+_1)}{B(E1;1^-_{\mathrm{ms}}\to 0^+_1)} = \frac{6}{25}\frac{\chi^2}{N} = R_{1^-_1} \approx 2. \tag{7}$$

We stress that the U(5) dynamical symmetry limit with structural parameters $\chi_\pi = \chi_\nu = 0$ and our reasonable choice for the $E1$ transition operator predict identical $E1$ decay branching ratios, R_{1^-}, for the symmetric and mixed-symmetry quadrupole-octupole coupled dipole excitations, 1_1^-, 1^-_{ms}, and $1^{-\prime}_{\mathrm{ms}}$. Beside the *structural* choice of the $E1$ operator, this prediction is independent of any model parameters in the U(5) limit. Breaking of the U(5) symmetry must be expected to destroy this equality of R_{1^-} values. A quantitative study of the individual evolution of R_{1^-} values with a breaking of the U(5) limit requires numerical diagonalizations of the *sdf*-IBM-2 Hamiltonian, which is outside of the scope of the present investigation. Indeed, we test the validity of the collective structure and do not intend to reproduce all correlations that lead to deviations.

Due to the many dipole excitations in the energy region of interest, lacking parity information complicates the identification of the 1^-_{ms} state in ^{142}Ce. Furthermore, decay branching ratios to higher excited states and the multipolarities of the corresponding transitions are widely unknown. For the 1^-_{ms} state the expected characteristic $E2$ and $M1$ transitions to the isoscalar 3_1^- and 1_1^- states, as well as the predicted $E1$ and $E3$ decays to the 1^+_{ms} and $2^+_{1,\mathrm{ms}}$ fragments, must be expected to disappear in the large nonresonant background at low energies.

Detailed branching ratios for four states in our data set are known from the previously mentioned β-decay experiments. We stress, however, that the data from NDS [36] are questionable. The decay pattern of the level at 2801 keV [36] disagrees, for example, with our results and with the findings from Ref. [18]. Also the spin assignment $J=1$ for the level at 2365 keV is wrong, consistently demonstrated by Vanhoy *et al.* [18] and by our results. Therefore, we used only our data to determine the absolute transition strengths presented in Table II. Evaluators should be aware that any unobserved branch tends to increase the level widths extracted by us and thus reduces the actual level lifetimes. In the case of unknown parity we give the decay strengths for all possible (pure) multipolarities.

With exception of the 3515 keV level all the $J=1$ states between 3.3 and 3.9 MeV decay predominantly to the ground state (see Table I). Most transitions to the 2_1^+ are nonexisting or too weak for detection. As discussed above, the 1^-_{ms} state is expected to decay strongly to the 2_1^+ state with a branching ratio close to that one for the 1_1^- state. The only dipole excitation in ^{142}Ce showing a comparable branching ratio for the transitions to the 2_1^+ and 0_1^+ states is the level at 3515 keV with

$$R = \frac{B(E1;1^-\to 2^+_1)}{B(E1;1^-\to 0^+_1)} = 2.0(4), \tag{8}$$

assuming negative parity and pure $E1$ multipolarity. However, the absolute transition strength, $B(E1;1^-\to 0_1^+) = 0.15$

$\times 10^{-3}e^2$ fm^4, is about a factor of 3 lower than predicted by the model.

Nevertheless, we observe that only one of the dipole excitations shows a decay branching ratio as predicted for the $1^-_{\rm ms}$ state. An alternative $1^{-\prime}_{\rm ms}$ state is predicted to occur at about the same excitation energy with an identical $E1$ branching ratio, though with an $E1$ excitation strength more than an order of magnitude lower than for the $1^-_{\rm ms}$ state considered here. The data, hence, suggest the state at 3515 keV as a promising candidate for the isovector $(2^+_{\rm ms}\otimes 3^-_1)^{(1^-)}$ state. For an unambiguous identification we would need clearcut parity information and more data on the characteristic decay intensities to other excited states. That seems to be feasible only with the powerful tool of NRF using monoenergetic polarized photons [37] instead of a bremsstrahlung spectrum. A unambiguous identification of a two-phonon quadrupole-octupole-collective state with negative parity and mixed proton-neutron symmetry would be significant for the understanding of the proton-neutron degree of freedom on collective nuclear structures.

IV. CONCLUSION

We investigated dipole excitations in the near spherical nucleus ^{142}Ce with the method of nuclear resonance fluorescence using bremsstrahlung provided by the Stuttgart DYNAMITRON accelerator facility at 4.1 MeV end-point energy. Between 2.1 and 3.9 MeV, 14 excitations with $J=1$ have been observed, five of them for the first time. Only one of these newly discovered dipole excitations shows a branching ratio for the decays to the ground state and to the 2^+_1 state, meeting the expectations for the recently proposed $1^-_{\rm ms}$ state [15]. This state is a promising candidate for the dipole member of the $(2^+_{1,\rm ms}\otimes 3^-_1)^{(J^-)}$ quintuplet of mixed-symmetry states with negative parity, which establishes a new class of proton-neutron mixed-symmetry states described within the sdf-IBM-2. A schematic description within the pure U(5) dynamical symmetry limit has been used for reproducing known states with positive and negative parity in ^{142}Ce in order to obtain a well-founded set of parameters for quantitative predictions of the decay pattern of the more exotic $1^-_{\rm ms}$ excitation. Given the choice of the two-body $E1$ transition operator of the sdf-IBM-2 in the literature, the U(5) limit predicts the $E1$ decay branching ratio $R_{1^-_{\rm ms}}$ to be equal to the corresponding branching ratio for the 1^-_1 state independent of any model parameter. The data for the $1^-_{\rm ms}$ candidate state at 3.5 MeV match this prediction within the error bars.

ACKNOWLEDGMENTS

The authors thank J. Jolie, T. Otsuka, A. Gelberg, T. Mizusaki, and P. van Isacker for valuable discussions. The authors from Köln thank the Institut für Strahlenphysik of the University Stuttgart for its kind hospitality during the NRF run. This work was partly supported by the Deutsche Forschungsgemeinschaft under Contract Nos. Br799/10–1, Kn154/30, Pi393/1–2 and by the NSF under Grant No. PHY–0245018.

[1] W. Andrejtscheff, C. Kohstall, P. von Brentano, C. Fransen, U. Kneissl, N. Pietralla, and H. H. Pitz, Phys. Lett. B **506**, 239 (2001).

[2] R.-D. Herzberg, I. Bauske, P. von Brentano, Th. Eckert, R. Fischer, W. Geiger, U. Kneissl, J. Margraf, H. Maser, N. Pietralla, H. H. Pitz, and A. Zilges, Nucl. Phys. **A592**, 211 (1995).

[3] J. Bryssinck, L. Govor, D. Belic, F. Bauwens, O. Beck, P. von Brentano, D. De Frenne, T. Eckert, C. Fransen, K. Govaert, R.-D. Herzberg, E. Jacobs, U. Kneissl, H. Maser, A. Nord, N. Pietralla, H. H. Pitz, V. Yu. Ponomarev, and V. Werner, Phys. Rev. C **59**, 1930 (1999).

[4] M. Wilhelm, E. Radermacher, A. Zilges, and P. von Brentano, Phys. Rev. C **54**, R449 (1996).

[5] M. Wilhelm, S. Kasemann, G. Pascovici, E. Radermacher, P. von Brentano, and A. Zilges, Phys. Rev. C **57**, 577 (1998).

[6] M. Babilon, T. Hartmann, P. Mohr, K. Vogt, S. Volz, and A. Zilges, Phys. Rev. C **65**, 037303 (2002).

[7] A. Gade, D. Belic, P. von Brentano, C. Fransen, H. von Garrel, J. Jolie, U. Kneissl, C. Kohstall, A. Linnemann, H. H. Pitz, M. Scheck, F. Stedile, and V. Werner, Phys. Rev. C **67**, 034304 (2003).

[8] N. Pietralla, C. Fransen, D. Belic, P. von Brentano, C. Friessner, U. Kneissl, A. Linnemann, A. Nord, H. H. Pitz, T. Otsuka, I. Schneider, V. Werner, and I. Wiedenhöver, Phys. Rev. Lett. **83**, 1303 (1999).

[9] N. Pietralla, C. Fransen, P. von Brentano, A. Dewald, A. Fitzler, C. Frießner, and J. Gableske, Phys. Rev. Lett. **84**, 3775 (2000).

[10] C. Fransen, N. Pietralla, P. von Brentano, A. Dewald, J. Gableske, A. Gade, A. Lisetskiy, and V. Werner, Phys. Lett. B **508**, 219 (2001).

[11] H. Klein, A. Lisetskiy, N. Pietralla, C. Fransen, A. Gade, and P. von Brentano, Phys. Rev. C **65**, 044315 (2002).

[12] A. Gade, H. Klein, N. Pietralla, and P. von Brentano, Phys. Rev. C **65**, 054311 (2002).

[13] V. Werner, D. Belic, P. von Brentano, C. Fransen, A. Gade, H. von Garrel, J. Jolie, U. Kneissl, C. Kohstall, A. Linnemann, A. F. Lisetskiy, N. Pietralla, H. H. Pitz, M. Scheck, K.-H. Speidel, F. Stedile, and S. W. Yates, Phys. Lett. B **550**, 140 (2002).

[14] C. Fransen, N. Pietralla, Z. Ammar, D. Bandyopadhyay, N. Boukharouba, P. von Brentano, A. Dewald, J. Gableske, A. Gade, J. Jolie, U. Kneissl, S. R. Lesher, A. F. Lisetskiy, M. T. McEllistrem, M. Merrick, H. H. Pitz, N. Warr, V. Werner, and S. W. Yates, Phys. Rev. C **67**, 024307 (2003).

[15] N. A. Smirnova, N. Pietralla, T. Mizusaki, and P. Van Isacker, Nucl. Phys. **A678**, 235 (2000).

[16] T. Otsuka, A. Arima, and F. Iachello, Nucl. Phys. **A309**, 1 (1978).

[17] N. Pietralla, C. Fransen, A. Gade, N. A. Smirnova, P. von Brentano, V. Werner, and S. W. Yates, Phys. Rev. C **68**, 031305(R) (2003).

[18] J. R. Vanhoy, J. M. Anthony, B. M. Haas, B. H. Benedict, B. T. Meehan, S. F. Hicks, C. M. Davoren, and C. L. Lundstedt,

Phys. Rev. C **52**, 2387 (1995).
[19] W. J. Vermeer, C. S. Lim, and R. H. Spear, Phys. Rev. C **38**, 2982 (1988).
[20] C. Fransen, O. Beck, P. von Brentano, T. Eckert, R.-D. Herzberg, U. Kneissl, H. Maser, A. Nord, N. Pietralla, H. H. Pitz, and A. Zilges, Phys. Rev. C **57**, 129 (1998).
[21] U. Kneissl, H. H. Pitz, and A. Zilges, Prog. Part. Nucl. Phys. **37**, 349 (1996).
[22] R. H. Spear, W. J. Vermeer, S. M. Burnett, G. J. Gyapong, and C. S. Lim, J. Phys. (Paris) **42**, 1427 (1989).
[23] E. Michelakakis, W. D. Hamilton, P. Hungerford, G. Jung, B. Pfeiffer, and S. M. Scott, J. Phys. G **8**, 111 (1982).
[24] A. L. Lapolli, C. B. Zamboni, and R. N. Saxena, Phys. Rev. C **41**, 2312 (1990).
[25] W. Kim, J. R. Calarco, J. P. Connelly, J. H. Heisenberg, F. W. Hersman, T. E. Milliman, J. E. Wise, B. L. Miller, C. N. Papanicolas, V. Yu. Ponomarev, E. E. Saperstein, and A. P. Platonov, Phys. Rev. C **44**, 2400 (1991).
[26] N. Pietralla, I. Bauske, O. Beck, P. von Brentano, W. Geiger, R.-D. Herzberg, U. Kneissl, J. Margraf, H. Maser, H. H. Pitz, and A. Zilges, Phys. Rev. C **51**, 1021 (1995).
[27] T. Eckert, O. Beck, J. Besserer, P. von Brentano, R. Fischer, R.-D. Herzberg, U. Kneissl, J. Margraf, H. Maser, A. Nord, N. Pietralla, H. H. Pitz, S. W. Yates, and A. Zilges, Phys. Rev. C **56**, 1256 (1997); **57**, 1007 (1998).
[28] F. Iachello and A. Arima, *The Interacting Boson Model* (Cambridge University Press, Cambridge, 1987).
[29] D. Bohle, A. Richter, W. Steffen, A. E. L. Dieperink, N. Lo Iudice, F. Palumbo, and O. Scholten, Phys. Lett. **137B**, 27 (1984).
[30] A. Richter, Prog. Part. Nucl. Phys. **34**, 261 (1995).
[31] N. Pietralla, P. von Brentano, R.-D. Herzberg, U. Kneissl, N. Lo Iudice, H. Maser, H. H. Pitz, and A. Zilges, Phys. Rev. C **58**, 184 (1998).
[32] J. Enders, H. Kaiser, P. von Neumann-Cosel, C. Rangacharyulu, and A. Richter, Phys. Rev. C **59**, R1851 (1999).
[33] A. A. Kuliev, E. Gulliyev, and M. Gerçeklioğlu, J. Phys. G **28**, 407 (2002).
[34] N. Lo Iudice and Ch. Stoyanov, Phys. Rev. C **65**, 064304 (2002).
[35] W. D. Hamilton, A. Irbäck, and J. P. Elliott, Phys. Rev. Lett. **53**, 2469 (1984).
[36] L. K. Peker, Nucl. Data Sheets **63**, 647 (1991).
[37] N. Pietralla, Z. Berant, V. N. Litvinenko, S. Hartmann, F. F. Mikhailov, I. V. Pinayev, G. Swift, M. W. Ahmed, J. H. Kelley, S. O. Nelson, R. Prior, K. Sabourov, A. P. Tonchev, and H. R. Weller, Phys. Rev. Lett. **88**, 012502 (2002).